The EMBO Journal vol.15 no.19 pp.5290–5298, 1996

Oncoprotein 18 is a phosphorylation-responsive regulator of microtubule dynamics

Ulrica Marklund, Niklas Larsson, Helena Melander Gradin, Göran Brattsand[1] and Martin Gullberg[2]

Departments of Cell and Molecular Biology and [1]Pathology, University of Umeå, S-901 87 Umeå, Sweden

[2]Corresponding author

Oncoprotein 18 (Op18, also termed p19, p18, prosolin or stathmin) is a cytosolic protein of previously unknown function. Phosphorylation of Op18 is cell cycle regulated by cyclin-dependent kinases (CDKs), and expression of a 'CDK target site-deficient mutant' results in a phenotype indicative of a role for Op18 during mitosis. This phenotype is compatible with the idea that Op18 is a phosphorylation-responsive regulator of microtubule (MT) dynamics. Therefore, in this study, we analyzed MTs in cells induced to express either wild-type or mutated Op18. The results showed that wild-type Op18 and a CDK target site mutant both efficiently elicited rapid depolymerization of MTs. This result contrasts with clear-cut differences in their cell cycle phenotypes. Morphological analysis of MTs explained this apparent discrepancy: while interphase MTs were depolymerized in cells expressing either Op18 derivative, apparently normal mitotic spindles were formed only in cells overexpressing wild-type Op18. This result correlates with our finding that only mutated Op18 causes a block during mitosis. Hence, we conclude that Op18 decreases MT stability and that this activity of Op18 is subject to cell cycle regulation by CDKs.

Keywords: cell cycle/cyclin-dependent kinases/microtubule/oncoprotein 18/stathmin

Introduction

Oncoprotein 18 (Op18) is a conserved cytosolic protein that has been studied independently in various cellular systems as p19, 19K, p18, prosolin, stathmin and Op18 (Doye *et al.*, 1989; Schubart *et al.*, 1989; Zhu *et al.*, 1989; Cooper *et al.*, 1990; Gullberg *et al.*, 1990). Op18 was identified initially due to its complex pattern of phosphorylation in response to activating signals and elevated expression in acute leukemias. This protein is expressed in great abundance (up to 5×10^6 molecules per cell) in various types of neoplasm (Hanash *et al.*, 1988; Brattsand *et al.*, 1993; Roos *et al.*, 1993; Friedrich *et al.*, 1995), and we have therefore adopted the designation Op18 (Melhem *et al.*, 1991).

Op18 is phosphorylated on four residues in intact cells, namely Ser16, Ser25, Ser38 and Ser63 (Labdon *et al.*, 1992; Beretta *et al.*, 1993; Marklund *et al.*, 1993a,b, 1994a; Luo *et al.*, 1994). The complex pattern of phosphorylation in response to a multitude of external signals (Cooper *et al.*, 1990; Doye *et al.*, 1990) prompted our previous site mapping studies that demonstrated phosphorylation of Op18 on Ser16 and Ser25 by two distinct protein kinases. Analysis after stimulation of the T-cell antigen receptor revealed that Ser25 is a target for members of the mitogen-activated protein (MAP) kinase family (Marklund *et al.*, 1993a,b) and that Ser16 is a target for the Ca^{2+}/calmodulin-dependent kinase IV/Gr (Marklund *et al.*, 1994a).

Recent studies have shown that phosphorylations of all four serine residues fluctuate during the cell cycle (Brattsand *et al.*, 1994; Luo *et al.*, 1994; Larsson *et al.*, 1995). Site mapping studies identified cyclin-dependent kinases (CDKs) as the kinase system involved in cell cycle-regulated phosphorylation of Ser25 and Ser38, but the cell cycle-regulated kinase system(s) involved in Ser16 and Ser63 phosphorylation remains to be identified (Marklund *et al.*, 1993b; Brattsand *et al.*, 1994). Phosphorylation of the two Op18 CDK target sites increases during S-phase progression, and at mitosis these two sites are phosphorylated to completion (Brattsand *et al.*, 1994; Larsson *et al.*, 1995). Since Ser16 and Ser63 are also phosphorylated extensively during mitosis, although not to completion, Op18 is one of the major mitotic phosphorylation substrates in many cell types.

To investigate the function of Op18, we recently have expressed 'phosphorylation target site-deficient mutants' of Op18 and searched for defects at the level of cell cycle regulation (Marklund *et al.*, 1994b; Larsson *et al.*, 1995). The results demonstrated that induced ectopic expression of an Op18 mutant, substituted at its two CDK target sites, results in accumulation of cells with a G_2/M content of DNA. The block during cell division was transient, and prolonged culture resulted in a large fraction of the transfected cells entering S-phase in the absence of mitosis, i.e. endoreduplication. Interestingly, the same phenotype was observed after mutation of the two 'non-CDK' sites, namely Ser16 and Ser63 (Larsson *et al.*, 1995). Thus, it appears that cell division requires multi-site phosphorylation of Op18 by at least two distinct protein kinase systems.

As outlined above, the phenotype of 'kinase site-deficient' mutants is compatible with a phosphorylation-regulated role for Op18 at the level of microtubule (MT) dynamics. Moreover, shortly before completion of the present study, Op18 was identified as a factor that alters MT dynamics *in vitro* and in *Xenopus* egg extracts (Belmont and Mitchison, 1996). In the present study, we have evaluated a potential MT-regulating role for Op18 by analyzing the MT content, morphology and cell cycle phenotype of cells induced to express wild-type Op18, an inactive deletion derivative or a 'CDK target site-deficient' mutant.

Results

Induced expression of a CDK target site-deficient mutant of Op18 results in a phenotype indistinguishable from the effect of drugs that interfere with MT dynamics

To express Op18 wild-type (Op18-wt) and the growth-inhibitory CDK target site-deficient Op18-S25,38A mutant, we employed the episomal Epstein–Barr virus (EBV)-based vector pMEP4. Using a specifically formulated growth medium, the hMTIIa promoter of this vector can be suppressed efficiently by non-toxic levels of EDTA or induced rapidly within 2–4 h in the presence of Cd^{2+} (see Materials and methods and below). Figure 1A shows a time course of changes in the DNA profile after induced expression of the indicated pMEP4 derivative. The data reveal rapid accumulation of cells with a G_2/M content of DNA in cultures induced to express Op18-S25,38A, while the DNA profile of cells expressing Op18-wt was only moderately changed compared with the vector control. Interestingly, the rate at which cells accumulated in the G_2/M phase of the cell cycle in the presence of the MT-depolymerizing drug nocodazole was essentially the same as that observed after induced expression of the Op18-S25,38A mutant.

Using the MPM-2 monoclonal antibody in combination with flow cytometry, the fraction of mitotic cells within the G_2/M (4N) peak can be quantified (Davis *et al.*, 1983; Landberg *et al.*, 1990). The result in Figure 1B shows that induced expression of the Op18-S25,38A mutant, or addition of nocadozole to vector control cells, results in a rapid accumulation of mitotic cells. In contrast, induced expression of Op18-wt only results in a minor effect compared with the vector control. Remarkably similar effects were achieved by expression of the Op18-S25,38A mutant and treatment of vector control cells with nocadozole. Thus, at the 22 h time point, ~60–70% of all cells within the G_2/M peak are arrested in mitosis, and thereafter the fraction of mitotic cells decreases. Hence, the mitotic block that results from either expression of Op18-S25,38A or disruption of MTs is transient in the K562 leukemia cell line.

Entry into mitosis is associated with a burst of CDK activation, mainly of the type cyclin B-associated p34-cdc2 kinase, and kinase activity is turned off at the metaphase–anaphase transition (Glotzer *et al.*, 1991; Norbury and Nurse, 1992). To analyze CDK activity in transfected cells, cell extracts were prepared after 24 h of induced expression in the presence or absence of nocodazole. Kinase activities in cell extracts were analyzed by using two distinct substrate peptides designed to be specific for either CDKs or, as a control, for members of the MAP kinase family. Figure 1C, lower histogram, shows that, as expected, neither nocadozole treatment nor induced expression of Op18 alters the level of MAP kinase activity. Nocodazole treatment of vector control cells resulted in the expected 6- to 7-fold increase in total CDK activity as a result of accumulation of cells blocked in metaphase. Importantly, similar levels of CDK activity were recovered from cells that are blocked in mitosis as a result of expressing the Op18-S25,38A mutant. Further nocodazole treatment has only a minor augmenting effect. Finally, expression of Op18-wt did not result in a significant increase in CDK activity, but CDK activity was still induced efficiently in the presence of nocadozole. Thus, cells arrested in mitosis by either Op18-S25,38A or drug-induced depolymerization of MT contain similar levels of CDK activity.

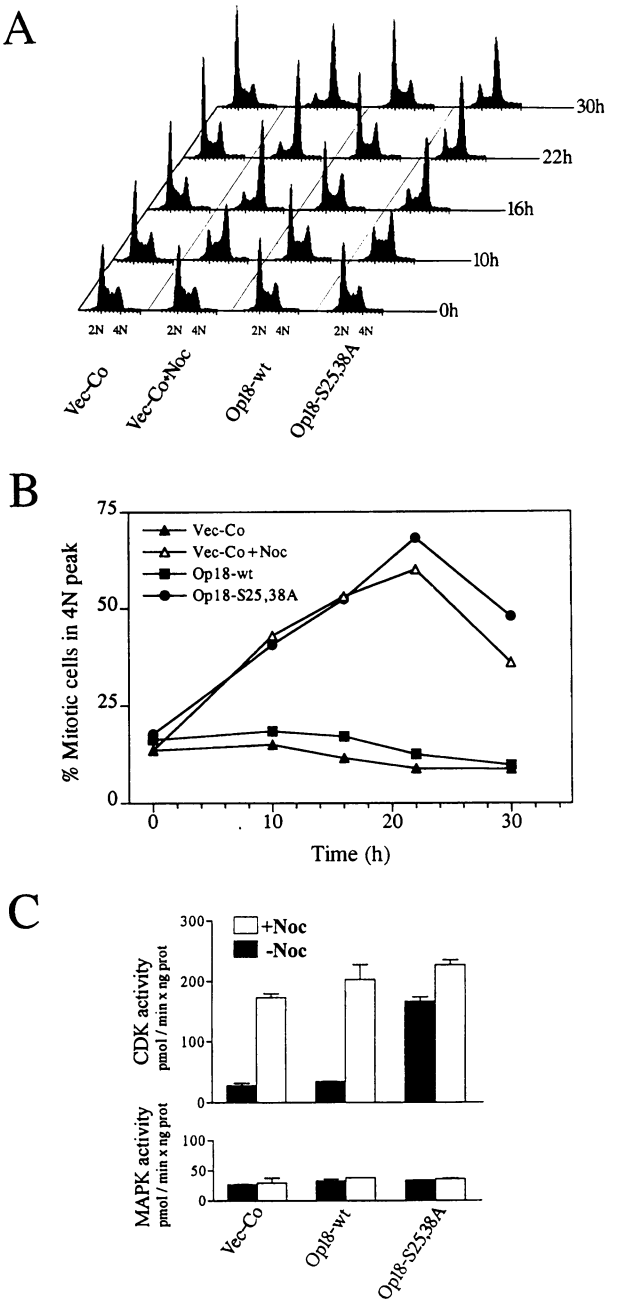

Fig. 1. A transient metaphase block in cells expressing a CDK target site-deficient mutant of Op18. K562 cells were transfected with pMEP4 (Vec-Co,▲), pMEP-Op18-wt (Op18-wt,■) or pMEP-Op18-S25,38A (Op18-S25,38A, ●) and hygromycin-resistant cell lines were selected as described in Materials and methods. Thereafter, cells were treated with Cd^{2+} (0.1 μM) to induce expression from the hMTIIa promotor. Vec-Co cells treated with 500 nM nocadozole (Vec-Co + Noc, △) are also shown. (**A**) DNA profiles were determined after the indicated time. (**B**) DNA and MPM-2 dual parameter staining of the same cell population as (A). Data are expressed as the percentage of MPM-2-positive (mitotic) cells within the 4N DNA peak. (**C**) Total CDK (upper histogram) and MAP kinase (lower histogram) activities in 5 μg of cell extracts derived from the indicated transfected cell population induced for 24 h with Cd^{2+} (0.1 μM), in the absence (closed bars) or presence (open bars) of 500 nM nocodazole.

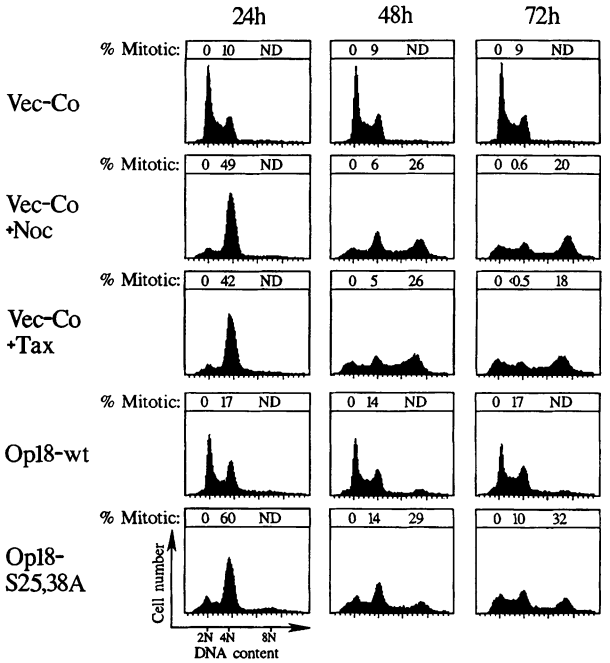

Fig. 2. Long-term effect on DNA content and frequency of cells in mitosis. K562 cells were transfected with the indicated pMEP4 derivative, and hygromycin-resistant cell lines were selected as in Figure 1. Thereafter, cells were treated with Cd^{2+} (0.1 μM) and DNA profiles were analyzed at 24, 48 and 72 h as indicated. Vector control cells (Vec-Co) were also treated with either nocadozole (Noc, 500 nM) or taxol (Tax, 1 μM) as indicated. DNA and MPM-2 dual parameter staining was also performed, and the data are expressed as the percentage of MPM-2-positive (% mitotic) cells in the 4N and 8N DNA peak (at the top of each histogram).

We have shown previously, using leukemic K562 cells, that mutated Op18 causes an immediate accumulation of cells with a G_2/M content of DNA and that prolonged expression results in a fraction of cells entering S-phase in the absence of cell division (Marklund *et al.*, 1994b). The results in Figure 2 show the long-term effect of Op18-S25,38A expression compared with the effect of treatment of vector control cells with either the MT-depolymerizing drug nocadozole or with the MT-stabilizing drug taxol. Interestingly, the DNA profiles reveal that 48–72 h of nocodazole or taxol treatment results in a similar degree of endoreduplication as expression of the Op18 mutant. Moreover, determination of MPM-2-positive cells in the 4N peaks revealed a similar and transient accumulation of mitotic cells that peaks after 24 h of drug treatment/induced expression (Figure 2, see top of each histogram). Later time points show accumulation of mitotic cells at the 8N peak, which implies cell cycle progression in the absence of cell division. In agreement with the result in Figure 1, the effect of ectopic Op18-wt expression was modest compared with the CDK target site-deficient mutant. In conclusion, the result in Figures 1 and 2 reveals similarities in the cell cycle block caused by Op18-S25,38A and two distinct drugs that disrupt MT function. In all cases, it appears that cells are transiently blocked in mitosis and that a fraction of these cells proceeds into the next cell cycle in the absence of cell division.

Modulation of the G_2/M phenotype of Op18 by nocodazole and taxol

The result outlined above suggested that Op18 expression may interfere with MT dynamics. If this is the case, then nocadozole and taxol, at concentrations sufficiently low to not cause mitotic arrest, would be expected to either enhance or suppress the phenotype depending on how Op18 modulates MT stability. Accordingly, the effect on cells induced to express the empty vector, Op18-wt or Op18-S25,38A in the presence or absence of either nocodazole (30 nM) or taxol (2 nM) was evaluated (see Figure 3). These concentrations were sufficiently low to not alter the DNA profile significantly in cells containing vector control (Figure 3A). Interestingly, addition of 30 nM nocadozole enhanced the slight increase of cells with a G_2/M content of DNA caused by 24 h expression of Op18-wt, while 2 nM taxol was without detectable effect. Conversely, the DNA profile of cells expressing Op18-S25,38A revealed the characteristic accumulation of cells in the G_2/M peak, and this phenotype appeared partially suppressed in the presence of 2 nM taxol, while nocadozole was without effect. Taxol-dependent suppression of the phenotype was also evident at the level of cell proliferation. The data in Figure 3B show that treatment of cells expressing Op18-S25,38A with 2 nM taxol results in almost a doubling of [^{3}H]thymidine incorporation, while a 25% decrease was evident among vector control cells. In conclusion, the weak G_2/M block phenotype caused by expression of Op18-wt is enhanced by 30 nM nocodazole, while the strong G_2/M block phenotype caused by Op18-S25,38A is partially suppressed by 2 nM taxol.

Ectopic expression of Op18 depolymerizes MTs

The simplest interpretation of the results outlined in Figure 3 is that expression of Op18 promotes depolymerization of MTs and that mutation of the CDK target sites modulates this function. We therefore examined the degree of polymerized tubulin in transfected cells by extracting soluble tubulin in an MT-stabilizing buffer (see Materials and methods). The particulate cytoskeleton (P) and soluble (S) fractions were separated by SDS–PAGE, and α-tubulin was immunodetected to determine the relative content of polymerized tubulin (Figure 4A). The data revealed that 24 h of either Op18-wt or Op18-S25,38A expression results in a drastic decrease of MTs in the particulate fraction. It appears that Op18 elicits depolymerization without direct interaction with MTs, since both the endogenous and ectopically expressed gene products are recovered solely in the soluble fraction (Figure 4A, lower panels). Moreover, from the data depicted in Figure 4B, which shows quantification of the tubulin ratio in the particulate and soluble fractions, it is evident that both Op18 derivatives partially antagonize the stabilizing effect of taxol at 20 nM and enhance nocadozole-dependent depolymerization of MTs.

The observed effect of Op18 expression on MT dynamics could either be a slow adaptation process occurring during the 24 h of induced expression or a rapid response to the expression of Op18 protein. This question was addressed by correlating the kinetics of expression of Op18 with depolymerization of MTs. The data in Figure 4C show that both Op18-wt and Op18-S25,38A are expressed rapidly after addition of Cd^{2+} (dashed lines), resulting in 6- to 8-fold higher levels of the recombinant proteins as compared with the endogenous Op18. Most importantly, it is also evident that MT depolymerization in response to expressed Op18 is rapid, and that pronounced

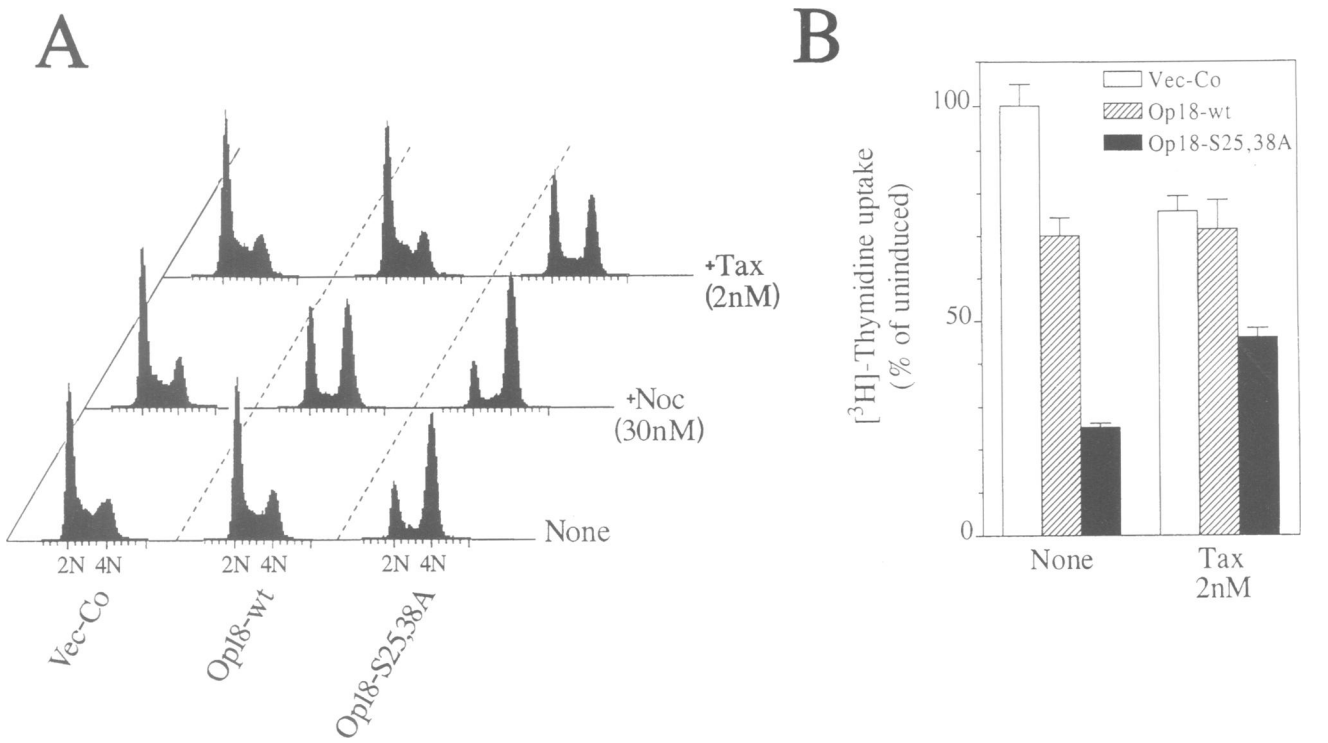

Fig. 3. Modulation of the Op18-mediated phenotype by drug-induced MT depolymerization/stabilization. (**A**) K562 cells were transfected with the indicated pMEP4 derivative, and hygromycin-resistant cell lines were selected as in Figure 1. Thereafter, cells were treated with Cd^{2+} (0.1 μM), in the absence or presence of either nocadozole (Noc, 30 nM) or taxol (Tax, 2 nM) as indicated, and DNA profiles were analyzed after 24 h. (**B**) [^{3}H]Thymidine incorporation into cells transfected and induced with Cd^{2+} as above. Cells were cultured for 24 h (2×10^4 cells/well), in the presence or absence of taxol as indicated. Data are presented as the percentage incorporation relative to EDTA-suppressed cells.

depolymerization has already occurred at the 2 h time point. It is notable that the level of ectopic Op18 at this early time point is modest and in the range of endogenous Op18.

The result in Figure 4A–C shows that both wild-type and the CDK target site-deficient Op18 protein can induce a rapid and dramatic depolymerization of MTs. However, it is also clear that expression of the Op18 mutant is somewhat more potent than that of the wild-type. For example, during the time course shown in Figure 4C, the differences between the wild-type and the mutant are clearly seen for the first 2 h. Thereafter, expression of the Op18 mutant caused an almost complete disintegration, while cells expressing Op18-wt retain a low, but significant, level of MTs. To determine if the difference in potency could be due to the phosphorylation status of the expressed Op18 proteins, phosphoisomers of Op18 were separated using a native PAGE system (Figure 4D). The data show that only 15% of endogenous Op18 was phosphorylated under the conditions used, with no detectable phosphorylation of more than a single site per molecule. Importantly, however, 67% of the overexpressed Op18-wt protein was found to be phosphorylated on up to four different sites, while analysis of the mutated Op18-S25,38A protein revealed that only 25% was phosphorylated. Hence, expression of Op18-S25,38A results in a higher number of unphosphorylated Op18 molecules per cell as compared with the wild-type derivative, which may explain differences in the potency of the expressed proteins in eliciting depolymerization of MTs. Hyperphosphorylation of overexpressed Op18 is reproducible and has been noted by us in a previous report (Larsson *et al.*, 1995), but the mechanism is at present unknown.

It has been proposed previously by others that Op18 is composed of a putative N-terminal regulatory region (amino acids 5–62), containing the two CDK target sites, and a C-terminal α-helical protein interaction region (Okazaki *et al.*, 1993; Maucuer *et al.*, 1995). Since deletion of amino acids 4–55 abolishes the cell cycle phenotype of the Ser63 mutation, it was of interest to determine if the same deletion (Op18-Δ4–55) also abolishes the MT-destabilizing activity of Op18 (Larsson *et al.*, 1995). As shown in Figure 5A, expression of Op18-Δ4–55 does not cause any significant alteration in the degree of MT polymerization, which is in agreement with the cell cycle phenotype (Larsson *et al.*, 1995), and suggests an essential role for the deleted region. However, this internally deleted Op18 protein was found to be expressed at only ~50% of the level of full-length Op18, which made comparison of the phenotype difficult (compare data in Figure 4C with Figure 5B). To evaluate the effect of Op18-wt expressed at levels similar to Op18-Δ4–55, we took advantage of the destabilizing effect of a Flag epitope tag attached to the C-terminus of Op18-wt (Op18-wt-Flag) (Marklund *et al.*, 1994b). Quantification of expression levels (Figure 5B) shows that the induced levels of the Op18-wt-Flag were somewhat lower than of the Op18-Δ4–55 protein. Importantly, the data show that even the modest expression level of Op18-wt-Flag, which is only 2- to 3-fold higher than expression of endogenous Op18, results in a drastic depolymerization response of MTs.

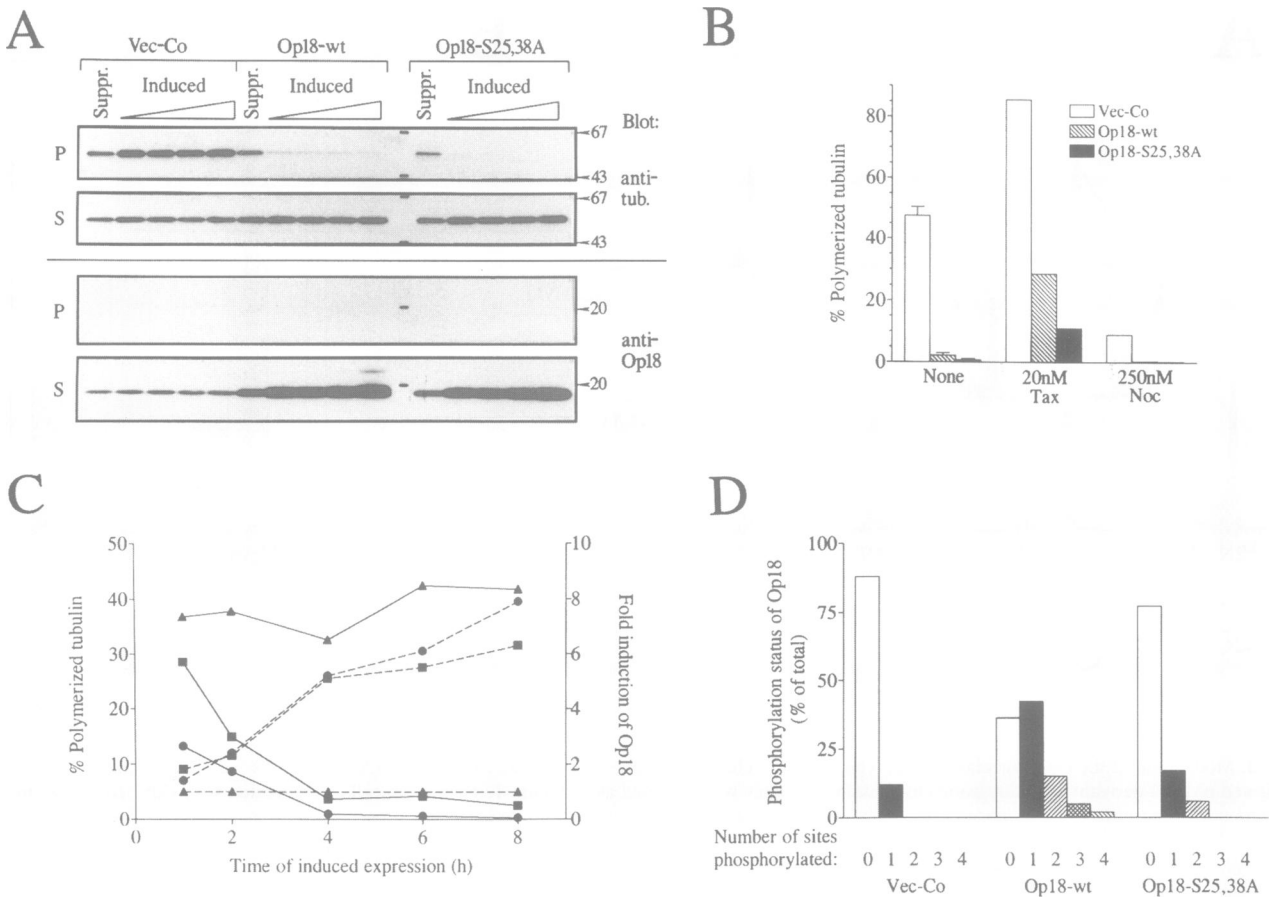

Fig. 4. Depolymerization of MTs by ectopic Op18 expression. (**A**) K562 cells were transfected with the indicated pMEP4 derivative, and hygromycin-resistant cell lines were selected as in Figure 1. Thereafter, cells were either suppressed by the presence of 25 μM EDTA or treated for 24 h with graded concentrations of Cd^{2+} (0.01, 0.03, 0.1 and 0.4 μM). Cells were then extracted with an MT-stabilizing buffer and the particulate (P) and soluble (S) fractions were prepared and analyzed as described in Materials and Methods. An autoradiograph of a Western blot analysis probed with either anti-α-tubulin (upper two panels) or anti-Op18 (lower two panels) and revealed with [^{125}I]protein A is shown. It should be noted that double the amount of cell equivalents is loaded for the particulate fractions, as compared with the soluble fractions. (**B**) Cells transfected as above were treated with either nocadozole (Noc) or taxol (Tax) during the last 3 h of a 7 h period of induced expression with 0.4 μM Cd^{2+}. Tubulin recovered in the particulate and soluble fractions was analyzed by quantitative Western blot analysis. The data are expressed as the percentage polymerized tubulin in the total cellular tubulin content, with the assumption that tubulin recovered in the particulate fraction represents MTs. (**C**) K562 cells, transfected with pMEP4 (▲), pMEP-Op18-wt (■) or pMEP-Op18-S25,38A (●), were treated with 0.1 μM Cd^{2+} for the indicated time and the MT content was quantified as in (B) (solid lines). Op18 levels were also determined by quantitative Western blot analysis (dashed lines) and data are presented as fold induction over endogenous Op18. (**D**) The indicated transfected cell lines were treated with 0.1 μM Cd^{2+} for 7 h and phosphoisomers of Op18 were resolved and quantified as described in Materials and Methods (up to four Ser sites, namely Ser16, Ser25, Ser38 and Ser63, are phosporylated *in vivo*).

Ectopic expression of Op18-wt depolymerizes MTs in interphase but not mitotic cells

Previous reports (Marklund *et al.*, 1994b; Larsson *et al.*, 1995) and the results in Figures 1–3 demonstrate that specific mutants of Op18 cause a complete block in cell division, while the cell cycle phenotype caused by overexpression of the wild-type protein is almost undetectable. An obvious question is how these data can be reconciled with the potent MT-depolymerizing effect of both Op18-wt and Op18-S25,38A shown in Figure 4A–C. To address this question, we analyzed the effect of expressed Op18 protein on MT morphology in interphase and mitotic cells. Accordingly, cells were extracted with an MT-stabilizing buffer, to remove free tubulin dimers, fixed and thereafter stained with an anti-α-tubulin antibody. The immunofluorescence shown in Figure 6A demonstrated a characteristic network of MTs in all of the interphase cells harboring the vector control. Moreover, as expected from the result in Figure 4, among the interphase cells that were induced for 5 h to express either Op18-wt or Op18-S25,38A, staining by anti-α-tubulin was almost undetectable. Importantly, however, functional mitotic spindles were observed at the expected frequency of ~5% among Op18-wt-expressing cells, but not among cells expressing Op18-S25,38A. Representative examples of spindles in vector-Co- and Op18-wt-transfected cells during metaphase or anaphase are shown in Figure 6B. In the case of Op18-S25,38A-transfected cells, about half of the mitotic cells lacked detectable MTs and their chromosomes appeared aggregated (note that the transgene was induced for 22 h, which results in a mitotic block of Op18-S25,38A-expressing cells). The rest of the mitotic cells contained one or two distinct spindle poles with very short MT arms, and two representative examples of these aberrant mitoses are shown in Figure 6B. The presence of spindle poles with very short MT arms suggests that the CDK target site-deficient mutant caused an abnormal increase in MT dynamics during mitosis, which in turn

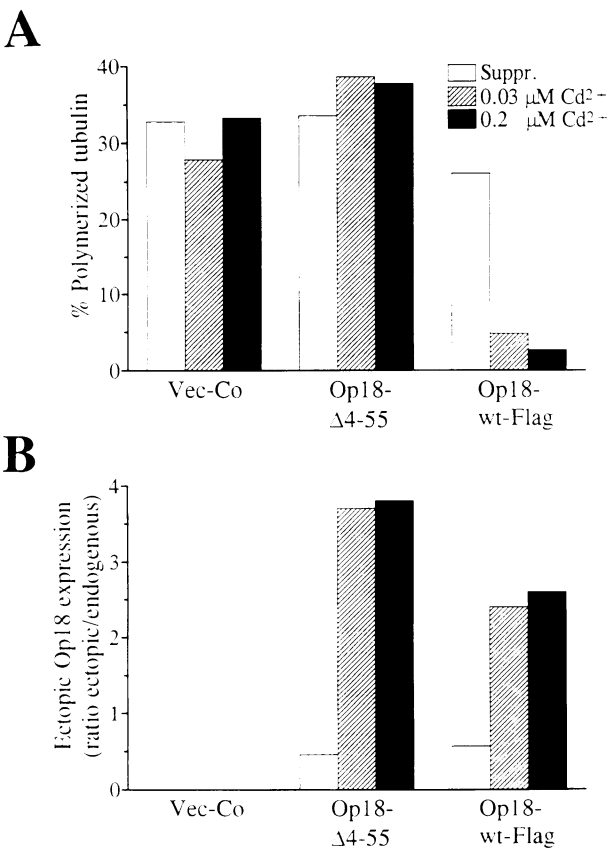

Fig. 5. Amino acids 4–55 of Op18 are essential for depolymerization of MTs. (**A**) K562 cells were transfected with pMEP4 (Vec-Co), pMEP-Op18-Δ4–55 (Op18-Δ4–55) or the epitope-tagged derivative pMEP-Op18-wt-Flag (Op18-wt-Flag). Hygromycin-resistant cell lines were selected as in Figure 1 and, thereafter, cells were either suppressed by the presence of 25 μM EDTA or treated for 7 h with the indicated concentrations of Cd^{2+}. Microtubule polymerization was analyzed and the data expressed as in Figure 4. Similar results were obtained after 4 and 24 h of induced expression. (**B**) Quantification by Western blot analysis of expressed Op18 after 7 h. The proteins encoded by Op18-Δ4–55 and Op18-wt-Flag migrate at 14 and 20.5 kDa, respectively, and are separated from endogenous Op18 by SDS–PAGE. The data are expressed as the ratio of ectopic Op18 relative to the level of the endogenous Op18.

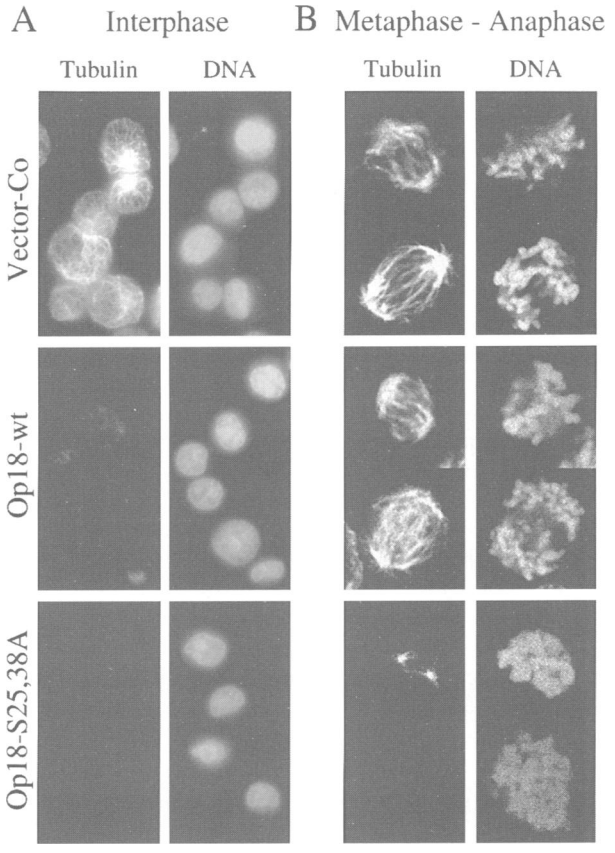

Fig. 6. Immunodetection of MTs in Op18-expressing cells. Cells transfected with the indicated pMEP4-based constructs were induced with Cd^{2+} for 5 h (**A**) or 22 h (**B**). Thereafter, cells were extracted with MT-stabilizing buffer, fixed and double stained with anti-α-tubulin and propidium iodide (DNA staining). (A) MT and DNA staining of representative interphase cells analyzed by epifluorescence, as indicated. (B) Examples of metaphase and anaphase cells observed using confocal microscopy among vector-Co- or Op18-wt-transfected cells or, in the case of Op18-S25,38A-transfected cells, two representative examples (with or without visible MT asters) of aberrant mitosis.

blocks formation of a functional mitotic spindle. This is in contrast to overexpression of Op18-wt, which abolishes the majority of interphase MTs but still allows cells to form functional mitotic spindles and to divide.

Discussion

Expression levels and phosphorylation of Op18 have been the subject of many previous studies, but the function of this protein has, until recently, been obscure. The first clue to the function of Op18 was provided by recent genetic approaches that suggested a role for Op18 during cell division (Marklund *et al.*, 1994b; Larsson *et al.*, 1995). It was shown that kinase target site-deficient mutants of Op18 caused an immediate accumulation of cells with a G_2/M content of DNA, followed by pronounced endoreplication. Morphological examination of cells arrested in G_2/M revealed that about one-third of the cells were arrested in mitosis, while the rest appeared as interphase cells. At that time, we interpreted the interphase morphology as an indication of a G_2 block. The present study shows that the phenotype observed upon expression of a CDK target site-deficient mutant is indistinguishable from the effect of drugs that either stabilize or depolymerize MT: each treatment causes a transient mitotic block in the K562 erythroleukemia cell line, which thereafter results in cells entering G_1 in the absence of cytokinesis and thus endoreduplication (Figures 1 and 2). This has prompted us to re-evaluate the nature of cells that we previously thought were blocked in G_2. Other studies have demonstrated that treatment of many tumor cell types with either nocodazole or taxol results in a phenomenon termed 'mitotic slippage' (Kung *et al.*, 1990; Rieder and Palazzo, 1992). This term implies that interference with the mitotic spindle results in a transient mitotic block and thereafter cells enter G1 without completing chromosome segregation and cell division, which results in subsequent endoreduplication. Taken together, the results in the present report show that, similarly to nocodazole and taxol treatment of K562 cells, ectopic expression of CDK target site-deficient mutants induces mitotic slippage that, in turn, results in generation of polyploid cells.

As outlined above, the cell cycle phenotype caused by expression of mutated Op18 may involve interference

with MT dynamics during formation of the mitotic spindle. This possibility gained further support by modulation of the cell cycle phenotype by either nocodazole or taxol. Thus, these two drugs, which have opposite effects on tubulin polymerization, either enhance or suppress the Op18-induced cell cycle phenotype, and the data suggest that Op18 expression elicits destabilization of MTs (Figure 3). Analysis of the polymerization status of MTs in intact cells confirmed this prediction: ectopic expression of both the wild-type and CDK target site-deficient mutant of Op18 results in depolymerization of MTs (Figure 4). The effect of induced expression of Op18 is rapid and, since depolymerization is almost complete within 4 h, we assume that the observed response occurs prior to any cell cycle block and that the readout of the assay mainly reflects the polymerization status among interphase cells. Moreover, Op18 appeared to be very efficient in mediating MT depolymerization, since ectopic expression levels that were only 2- to 3-fold higher than that of the endogenous protein were sufficient for 90% down-regulation of interphase MTs (Figure 5).

The cell cycle phenotype of mutated Op18 and the effect of drugs that interfere with MT dynamics appear indistinguishable. This can be explained readily by the observed depolymerizing activity of Op18. However, expression of wild-type Op18 was almost as efficient in depolymerizing MT as was that of the mutant (Figure 4), which contrasts the clear-cut differences in their cell cycle phenotype. A likely explanation for the difference between cells expressing wild-type and mutated Op18 becomes evident from a morphological analysis of MTs. As expected, most of the interphase MTs were depolymerized in cells expressing wild-type or mutated Op18, but cells expressing wild-type Op18 could form apparently normal mitotic spindles. In contrast, analysis of a cell population induced to express the Op18 mutant for 22 h, which results in a major mitotic block, failed to reveal functional mitotic spindles. Hence, while both the wild-type and mutated Op18 appear to have similar effects on interphase MTs, the data show that only mutated Op18 expression blocks formation of the mitotic spindle. It follows, therefore, that only mutated Op18 would cause a block during mitosis.

Before completion of this study, Op18 was identified by Belmont and Mitchison as a protein that increases the catastrophe rate of MTs during *in vitro* assembly (Belmont and Mitchison, 1996). Moreover, Op18 was found to interact with tubulin dimers, which the authors proposed may be of relevance for an MT-regulatory role for Op18. Identification of Op18 as a positive modulator of MT dynamics is certainly in line with the result from the present study; however, although the study of Belmont and Mitchison established that Op18 has the potential to regulate MT dynamics, its mechanism of action is still unknown. The results in this study illustrate some clear-cut differences between wild-type and a CDK target site-deficient mutant of Op18, which most likely reflects phosphorylation-dependent regulation of Op18 activity. Firstly, the cell cycle phenotype mediated by expression of mutated Op18 is strong, i.e. a complete mitotic block, while the effect of the same expression levels of wild-type Op18 is barely detectable. Secondly, ectopic expression of both wild-type and mutated Op18 results in depolymerization of MTs in interphase cells, but functional mitotic spindles are formed in cells expressing the wild-type derivative and these cells are able to divide. Finally, wild-type Op18 is less potent than the mutant in causing MT depolymerization in interphase cells, and this correlates with 2- to 3-fold increased phosphorylation of the over-expressed wild-type protein.

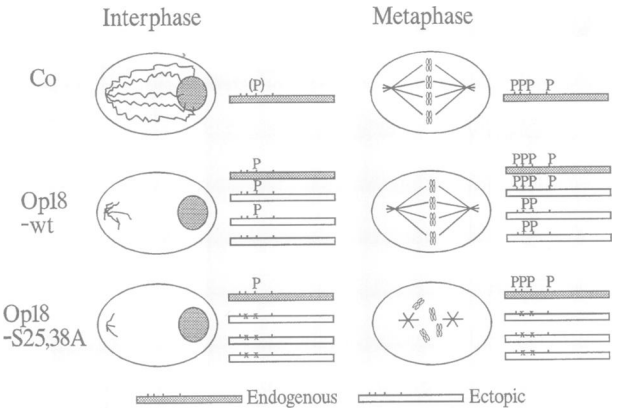

Fig. 7. Illustration of the observed phosphorylation status of Op18 in cells overexpressing either wild-type or a CDK target site-deficient mutant of Op18. Endogenous and ectopic Op18 are indicated by shaded and open bars, respectively. The number and position of phosphate groups (P) are based on the result in Figure 4D and the results of site mapping analysis in previous reports (Brattsand *et al.*, 1993; Larsson *et al.*, 1995). The P within brackets depicts the 10% stoichiometry of phosphorylation of endogenous Op18 observed in untransfected cells. The observed polymerization status of interphase and mitotic MTs in transfected cells is also illustrated.

The observations listed above are illustrated schematically in Figure 7, which depicts the phosphorylation status of Op18 in cells overexpressing either wild-type or the CDK target site-deficient mutant of Op18. The figure also illustrates our morphological observations on the status of interphase and mitotic MTs in transfected cells. The simplest interpretation of the observations summarized in Figure 7 is that phosphorylation may cause a general decrease in the potency with which expressed Op18 depolymerizes MT. Thus, assuming that phosphorylated Op18 protein is less active in depolymerizing MTs, hyperphosphorylation of overexpressed wild-type Op18 would explain its decreased activity compared with the mutant. The observed hyperphosphorylation of Op18 could suggest a feed-back mechanism that compensates for deleterious effects of overexpressed Op18 at the level of MT dynamics. Moreover, the finding that several-fold overexpression of wild-type Op18 does not cause a mitotic block also suggests that phosphorylation decreases the activity of Op18. Thus, during mitosis, cells may produce sufficient protein kinase activity to phosphorylate the overexpressed wild-type Op18 protein to the stoichiometry required to allow formation of a mitotic spindle; this would clearly be impossible in the case of the mutant. This would imply that cells can tolerate overexpression of Op18 during mitosis as long as sufficient kinase activity is available and all the sites for functional inhibitory phosphorylations are available. This interpretation may explain why over-expression of the wild-type Op18 protein is compatible with a functional mitotic spindle.

Our results suggest that phosphorylation of Op18 decreases its activity, and it follows that kinase target site-

deficient mutants of Op18 would be constitutively active. The frequently observed very short MT arms of the aberrant spindles in Op18-S25,38A-expressing cells (Figure 6) support such an interpretation. Constitutive activity is contrary to our initial proposal that the kinase target site-deficient mutants of Op18 act in a dominant-negative fashion in the G_2/M phase, i.e. the mutant proteins interfere with the function of the endogenous gene product. The strongest evidence for our initial proposal was that antisense mRNA-mediated suppression of Op18 expression results in a G_2/M block similar to Op18-S25,38A-expressing cells (Luo *et al.*, 1994; Marklund *et al.*, 1994b). However, recent data showed that immunodepletion of Op18 from *Xenopus* egg extracts caused an increase in polymerized tubulin (Belmont and Mitchison, 1996), which is opposite to the effect we observed in response to expression of mutated Op18. It follows that the G_2/M block induced by expression of antisense RNA is likely to be caused by an increase in polymerized tubulin, and not by depolymerization of MTs, i.e. the mechanism by which mutated Op18 causes a G_2/M block. Thus, it seems unlikely that CDK target site-deficient mutants of Op18 interfere with the function of the endogenous gene product and, as argued above, it seems more likely that mutation of the CDK phosphorylation sites abolishes negative regulation of its activity.

The present study suggests that Op18 phosphorylations on Ser25 and Ser38 by CDK during mitosis reduce the MT-destabilizing activity of Op18. This may appear contradictory to the simple model of Belmont and Mitchison (1996) whereby Op18 is proposed to be activated at the onset of mitosis by phosphorylation, to provide a mechanism for the observed increase in MT dynamics during mitosis. However, in addition to the two CDK phosphorylation sites, Op18 is also phosphorylated on Ser16 and Ser63 during mitosis (Larsson *et al.*, 1995). Hence, it remains possible that phosphorylation of Ser16 and Ser63 during mitosis, which is carried out by an as yet unidentified protein kinase, could either modulate or antagonize the effect of CDK phosphorylation on Ser25 and Ser38. A future challenge will be to elucidate how phosphorylation of specific sites, alone and in combination, modulates the activity of Op18 during interphase and mitosis.

Materials and methods

DNA constructs

DNA manipulations were performed by standard recombinant techniques (Sambrook *et al.*, 1989). Construction of the mutant Op18-S25,38A cDNA, where the codons for Ser25 and Ser38 are exchanged with Ala, and Op18-Δ4–55, where the sequence encoding amino acids 4–55 is deleted, have been described previously (Marklund *et al.*, 1994a). The nine amino acid Flag epitope tag (Hopp *et al.*, 1988) was fused to the COOH-terminal end of Op18-wt as described (Marklund *et al.*, 1994b). Op18 derivatives were isolated as *Bam*HI–*Hin*dIII fragments and cloned into the corresponding sites in the polylinker of the episomal EBV expression vector pMEP4 (Invitrogen) (Groger *et al.*, 1989).

DNA transfection, suppression of the hMTIIa promoter and cell culture conditions

The pMEP4-based plasmids described above allow expression of Op18 derivatives under control of the Cd^{2+}-inducible hMTIIa promoter. The pMEP4 shuttle vector contains the EBV origin of replication, the EBNA-1 gene to allow high-copy episomal replication, and the *hph* gene, which confers hygromycin B resistance in mammalian cells (Groger *et al.*, 1989). The K562 erythroleukemia cell line was transfected with pMEP-Op18 derivatives as described elsewhere (Marklund *et al.*, 1994b). In brief, K562 cells were transfected by electroporation in the presence of 12 μg of pMEP4-based derivatives, 5 μg of pCMV-EBNA and 25 μg of pBluescript SK(+) as carrier DNA. Cells thereafter were recultured in a medium containing EDTA (25 μM) which has been designed specifically to support cell growth under conditions that minimize expression from the hMTIIa promoter (Marklund *et al.*, 1994b). Hygromycin (0.5 mg/ml, Boehringer-Mannheim) was used to select for transfected cells, and ~50–70% of all pMEP4-transfected cells surviving electroporation were resistant to the drug, while essentially all mock-transfected cells were killed within 3 days. The experiments were performed routinely 5–6 days post electroporation.

Flow cytometric analysis and [^{3}H]thymidine incorporation

Single parameter DNA staining was performed with propidium iodide as described (Marklund *et al.*, 1994b). DNA and MPM-2 dual parameter stainings were performed on cells fixed in 70% ethanol buffered with 50 mM glycine buffer, pH 2 (–20°C). Cells were washed and incubated with a monoclonal antibody anti-MPM-2 (Landberg *et al.*, 1990) (Dakopatts A/S), which was revealed by fluorescein-conjugated rabbit anti-mouse immunoglobulin. Prior to analysis, cells were resuspended in phosphate-buffered saline (PBS) containing 10 μg/ml propidium iodide, 0.1% Triton X-100 and 10 μg/ml RNase. DNA and MPM-2 dual parameter analysis was performed using a FACScan (Becton Dickinson). Cellular proliferation was analyzed by culturing cells (0.2 ml/culture, triplicate cultures) in flat bottom microtiter plates in the presence of [^{3}H]thymidine (1 μCi/well) for 2 h. Cultures were thereafter terminated by precipitation on glass filters, and incorporation of [^{3}H]thymidine was determined by liquid scintillation.

Analysis of MT polymerization status, SDS–PAGE, Western blot and analysis of Op18 phosphoisomers

The extent of MT polymerization was determined by extracting soluble tubulin in an MT-stabilizing buffer essentially as described (Minotti *et al.*, 1991). The stabilizing buffer, which was sligthly modified, contained 0.1 M PIPES pH 6.9, 2 M glycerol, 5 mM $MgCl_2$, 2 mM EGTA, 0.5% Triton X-100, 4 mM taxol, 5 μg/ml pefablock and 5 μg/ml leupeptin. The tubulin content was analyzed in the particulate cytoskeleton and the soluble fractions by separation on a 10–20% gradient SDS–PAGE as described (Gullberg *et al.*, 1990). The tubulin content in each fraction was quantified by probing filters with anti-α-tubulin (clone B-5-1-2, Sigma). Bound antibodies were revealed by incubation with rabbit anti-mouse immunoglobulin followed by [^{125}I]protein A. PhosphorImager analysis of radioactive bands was used for quantification, and serial dilutions of samples were analyzed to ensure that the assays were performed in the linear range. Based on the assumption that tubulin recovered in the particulate fraction represents MT and that tubulin recovered in the soluble fraction represents free dimers, data are expressed as the percentage polymerized tubulin in the total cellular tubulin content. Affinity-purified anti-Op18, specific for the COOH-terminal (anti-Op18:34-149), was used for Western blot analysis together with [^{125}I]protein A as described (Brattsand *et al.*, 1993). As a control for equal loading, the relevant part of the filters was probed routinely with rabbit anti-triose phosphate isomerase or the PC10 monoclonal antibody. To separate Op18 phosphoisomers, we employed a native PAGE system that separates Op18 according to the charge differences introduced by each of the four identified phosphorylations, as previously described (Marklund *et al.*, 1993b).

Analysis of CDK and MAP kinase activity by in vitro phosphorylation

Cells were lysed in a Triton X-100-containing buffer as previously described (Marklund *et al.*, 1993b) and 5 μg (15 μl) of cellular protein was used for *in vitro* phosphorylation using either the cdc2 kinase enzyme assay system (Amersham) or the p42/p44 MAP kinase enzyme assay system (Amersham). The specificity of these two protein kinase assay systems relies on phosphorylation of specific substrate peptides, and the analyses were performed as recommended by the manufacture.

Immunofluorescence

Cells were extracted with MT-stabilizing buffer (see above) containing 0.05% saponin/10 μg/ml RNase. Cells were fixed in 4% paraformaldehyde/0.5% glutaraldehyde for 15 min followed by quenching with $NaBH_4$, and thereafter were stained with anti-α-tubulin (clone B-5-1-2, Sigma). Bound antibodies were revealed by fluorescein-conjugated rabbit anti-mouse immunoglobulin and DNA was stained with 0.1 μg/ml

propidium iodide. Cells were mounted using 1 mg/ml of *p*-phenylenediamine in PBS with 80% glycerol and analyzed by either epifluorescence or by using a Nikon Diaphot equipped with a Molecular Dynamics confocal imager system.

Acknowledgements

We thank Drs J.Raff and V.Shingler for critical reading of the manuscript, and Dr T.Mitchison for providing data while in press. This work was supported by the Swedish Natural Science Research Council, Lion's Cancer Research Foundation, University of Umeå (LP 797/91) and The Swedish Society for Medical Research.

References

Belmont,L.D. and Mitchison,T.J. (1996) Identification of a protein that interacts with tubulin dimers and increases the catastrophe rate of micotubule. *Cell*, **84**, 623–631.

Beretta,L., Dobransky,T. and Sobel,A. (1993) Multiple phosphorylation of stathmin. Identification of four sites phosphorylated in intact cells and *in vitro* by cyclic AMP-dependent protein kinase and p34cdc2. *J. Biol. Chem.*, **268**, 20076–20084.

Brattsand,G., Roos,G., Marklund,U., Ueda,H., Landberg,G., Nanberg,E., Sideras,P. and Gullberg,M. (1993) Quantitative analysis of the expression and regulation of an activation-regulated phosphoprotein (oncoprotein 18) in normal and neoplastic cells. *Leukemia*, **7**, 569–579.

Brattsand,G., Marklund,U., Nylander,K., Roos,G. and Gullberg,M. (1994) Cell-cycle-regulated phosphorylation of oncoprotein 18 on Ser16, Ser25 and Ser38. *Eur. J. Biochem.*, **220**, 359–368.

Cooper,H.L., Fuldner,R., McDuffie,E. and Braverman,R. (1990) A specific defect of prosolin phosphorylation in T cell leukemic lymphoblasts is associated with impaired down-regulation of DNA synthesis. *J. Immunol.*, **145**, 1205–1213.

Davis,F.M., Tsao,T.Y., Fowler,S.K. and Rao,P.N. (1983) Monoclonal antibodies to mitotic cells. *Proc. Natl Acad. Sci. USA*, **80**, 2926–2930.

Doye,V., Soubrier,F., Bauw,G., Boutterin,M.C., Beretta,L., Koppel,J., Vandekerckhove,J. and Sobel,A. (1989) A single cDNA encodes two isoforms of stathmin, a developmentally regulated neuron-enriched phosphoprotein. *J. Biol. Chem.*, **264**, 12134–12137.

Doye,V., Boutterin,M.C. and Sobel,A. (1990) Phosphorylation of stathmin and other proteins related to nerve growth factor-induced regulation of PC12 cells. *J. Biol. Chem.*, **265**, 11650–11655.

Friedrich,B., Gronberg,H., Landstrom,M., Gullberg,M. and Bergh,A. (1995) Differentiation-stage specific expression of oncoprotein 18 in human and rat prostatic adenocarcinoma. *Prostate*, **27**, 102–109.

Glotzer,M., Murray,A.W. and Kirschner,M.W. (1991) Cyclin is degraded by the ubiquitin pathway. *Nature*, **349**, 132–138.

Groger,R.K., Morrow,D.M. and Tykocinski,M.L. (1989) Directional antisense and sense cDNA cloning using Epstein–Barr virus episomal expression vectors. *Gene*, **81**, 285–294.

Gullberg,M., Noreus,K., Brattsand,G., Friedrich,B. and Shingler,V. (1990) Purification and characterization of a 19-kilodalton intracellular protein. An activation-regulated putative protein kinase C substrate of T lymphocytes. *J. Biol. Chem.*, **265**, 17499–17505.

Hanash,S.M., Strahler,J.R., Kuick,R., Chu,E.H. and Nichols,D. (1988) Identification of a polypeptide associated with the malignant phenotype in acute leukemia. *J. Biol. Chem.*, **263**, 12813–12815.

Hopp,T.P., Prickett,K.S., Price,V., Libby,R.T., March,C.J., Ceretti,P., Urdal,D.L. and Conlon,P.J. (1988) A short polypeptide marker sequence useful for recombinant protein identification and purification. *Bio/Technology*, **6**, 1205–1210.

Kung,A.L., Sherwood,S.W. and Schimke,R.T. (1990) Cell line-specific differences in the control of cell cycle progression in the absence of mitosis. *Proc. Natl Acad. Sci. USA*, **87**, 9553–9557.

Labdon,J.E., Nieves,E. and Schubart,U.K. (1992) Analysis of phosphoprotein p19 by liquid chromatography/mass spectrometry. Identification of two proline-directed serine phosphorylation sites and a blocked amino terminus. *J. Biol. Chem.*, **267**, 3506–3513.

Landberg,G., Tan,E.M. and Roos,G. (1990) Flow cytometric multiparameter analysis of proliferating cell nuclear antigen/cyclin and Ki-67 antigen: a new view of the cell cycle. *Exp. Cell Res.*, **187**, 111–118.

Larsson,N., Melander,H., Marklund,U., Osterman,O. and Gullberg,M. (1995) G2/M transition requires multisite phosphorylation of oncoprotein 18 by two distinct protein kinase systems. *J. Biol. Chem.*, **270**, 14175–14183.

Luo,X.N., Mookerjee,B., Ferrari,A., Mistry,S. and Atweh,G.F. (1994) Regulation of phosphoprotein p18 in leukemic cells. Cell cycle regulated phosphorylation by p34cdc2 kinase. *J. Biol. Chem.*, **269**, 10312–10318.

Marklund,U., Brattsand,G., Osterman,O., Ohlsson,P.I. and Gullberg,M. (1993a) Multiple signal transduction pathways induce phosphorylation of serines 16, 25, and 38 of oncoprotein 18 in T lymphocytes. *J. Biol. Chem.*, **268**, 25671–25680.

Marklund,U., Brattsand,G., Shingler,V. and Gullberg,M. (1993b) Serine 25 of oncoprotein 18 is a major cytosolic target for the mitogen-activated protein kinase. *J. Biol. Chem.*, **268**, 15039–15047.

Marklund,U., Larsson,N., Brattsand,G., Osterman,O., Chatila,T.A. and Gullberg,M. (1994a) Serine 16 of oncoprotein 18 is a major cytosolic target for the Ca^{2+}/calmodulin-dependent kinase-Gr. *Eur. J. Biochem.*, **225**, 53–60.

Marklund,U., Osterman,O., Melander,H., Bergh,A. and Gullberg,M. (1994b) The phenotype of a 'Cdc2 kinase target site-deficient' mutant of oncoprotein 18 reveals a role of this protein in cell cycle control. *J. Biol. Chem.*, **269**, 30626–30635.

Maucuer,A., Camonis,J.H. and Sobel,A. (1995) Stathmin interaction with a putative kinase and coiled-coil-forming protein domains. *Proc. Natl Acad. Sci. USA*, **92**, 3100–3104.

Melhem,R.F., Zhu,X.X., Hailat,N., Strahler,J.R. and Hanash,S.M. (1991) Characterization of the gene for a proliferation-related phosphoprotein (oncoprotein 18) expressed in high amounts in acute leukemia. *J. Biol. Chem.*, **266**, 17747–17753.

Minotti,A.M., Barlow,S.B. and Cabral,F. (1991) Resistance to antimitotic drugs in Chinese hamster ovary cells correlates with changes in the level of polymerized tubulin. *J. Biol. Chem.*, **266**, 3987–3994.

Norbury,C. and Nurse,P. (1992) Animal cell cycles and their control. *Annu. Rev. Biochem.*, **61**, 441–470.

Okazaki,T., Yoshida,B.N., Avraham,K.B., Wang,H., Wuenschell,C.W., Jenkins,N.A., Copeland,N.G., Anderson,D.J. and Mori,N. (1993) Molecular diversity of the SCG10/stathmin gene family in the mouse. *Genomics*, **18**, 360–373.

Rieder,C.L. and Palazzo,R.E. (1992) Colcemid and the mitotic cycle. *J. Cell Sci.*, **102**, 387–392.

Roos,G., Brattsand,G., Landberg,G., Marklund,U. and Gullberg,M. (1993) Expression of oncoprotein 18 in human leukemias and lymphomas. *Leukemia*, **7**, 1538–1546.

Sambrook,J., Fritsch,E.F. and Maniatis,T. (1989) *Molecular Cloning: A Laboratory Manual*. 2nd edn. Cold Spring Harbor Laboratory Press, Cold Spring Harbor, NY.

Schubart,U.K., Banerjee,M.D. and Eng,J. (1989) Homology between the cDNAs encoding phosphoprotein p19 and SCG10 reveals a novel mammalian gene family preferentially expressed in developing brain. *DNA*, **8**, 389–398.

Zhu,X.X. *et al.* (1989) Molecular cloning of a novel human leukemia-associated gene. Evidence of conservation in animal species. *J. Biol. Chem.*, **264**, 14556–14560.

Received on April 22, 1996; revised on June 11, 1996